Investigating the Uneven Current Injection in Perovskite-Based Thin Film Bipolar Resistance Switching Devices by Thermal Imaging

Zhi Luo[1], H. K. Lau[2], P. K. L. Chan[3] and C. W. Leung[2]

[1]Department of Electronic Engineering, Jinan University, Guangzhou 510632, China
[2]Department of Applied Physics, Hong Kong Polytechnic University, Hong Kong
[3]Department of Mechanical Engineering, University of Hong Kong, Hong Kong

Bipolar resistive switching (RS) phenomenon in planar Al/$Pr_{0.7}Ca_{0.3}MnO_3$ (PCMO)/Ti devices was investigated by thermoreflectance method. Thermal images of devices undergoing switching were used to quantify the unevenness of injected current under different voltage bias. At low resistance state, the injected current at the current crowding area of the Al/PCMO interface was 1.6 times higher than other regions of the interface. The uneven distribution of injected current indicated the existence of localized resistance at the interface, which cannot be simply measured by electrical measurements. The thermoreflectance method demonstrates the potential applications for *in situ* current profiling of the RS devices.

Index Terms—**Nonvolatile memories, $Pr_{0.7}Ca_{0.3}MnO_3$ (PCMO), resistive switching (RS), thermal imaging.**

I. Introduction

As THE demand on the data storage capacities for nonvolatile memories increases continuously, memory devices based on resistance switching (RS) have been studied vigorously since the last decade [1], [2]. RS devices incorporating solid electrolytes, organic molecules, or transition-metal oxides have been successfully demonstrated [3]–[5]. Among different RS devices, those with metal/oxide/metal planar and capacitor geometries have several outstanding advantages, including the low production cost, high chemical stability, and compatibility with flexible substrates [6].

For the oxide layer in such class of RS devices, both binary and perovskite oxides have been employed [7]–[10], and it has been shown that the RS mechanisms are different for devices with distinct structures and materials [11], [12]. Sawa *et al.* [13] proposed that the RS effect in capacitor-geometry RS devices originates from the Schottky barriers, with trapped charges present at the interface between the film material and the electrodes [14]. Using transverse electromagnetic, Li *et al.* [15] showed that a thin layer of AlO_x exists at the interface between the Al and $Pr_{0.7}Ca_{0.3}MnO_3$ (PCMO), and they proposed that the formation and dissociation of the AlO_x layer contributed to the RS effect in the perovskite oxide-based devices. On the other hand, the unipolar RS effect in binary oxide-based devices (such as nickel oxide) is believed to be related to the formation of conductive filamentary paths within the device [16], [17]. In particular, two types of unipolar RS effect (memory and threshold RS) have been reported, of which the threshold type is unsuitable for nonvolatile memory applications [16]. The threshold-type RS has not been reported so far in perovskite oxide-based bipolar RS devices.

Recently, we reported single-point (size ~ 30 μm) thermal measurements in Al/PCMO/Ni devices to investigate the RS phenomenon [18]. Our measurements showed an unequal heating at Al and Ni electrodes, and a larger temperature increase was observed at the Al electrodes when the device was switched from the high resistive state (HRS) to the low resistive state (LRS). At LRS, a larger current passes through the device, resulting in a stronger heating than HRS. The larger temperature rise at the Al electrode than the Ni electrode represents a larger series resistance exists at the Al side, given the identical current passing through the Al and Ni electrodes. Both the single-point thermal and electrical measurements suffer from the constraint of limited spatial resolution of the technique. The distribution of the resistance, and hence the uniformity of current injection into the RS devices, has not been completely studied.

In this paper, we take a step further by investigating the uniformity of the series resistance in between the PCMO and the metal electrodes of the planar RS device, using the nondestructive charge-coupled device (CCD)-based thermoreflectance method. Based on the thermal images, we quantified the current injected into the high temperature region during LRS is 60% more than the surrounding region. It provides direct evidence that localized resistance, hence uneven current injection, exists in the Al/PCMO interface of the RS device.

II. Materials and Method

2-D thermal images were obtained by CCD-based thermoreflectance; the technique has been previously applied for characterizing various electronic devices including semiconductor lasers, transistors, and amplifiers [19]–[21]. The schematic diagram of the thermoreflectance experimental setup is shown in Fig. 1(a). A 10× objective was used, yielding a spatial resolution of approximately 2 μm. By assuming a linear relationship between the changes of the reflectivity and the temperature, the temperature variation (ΔT) can be obtained by the thermoreflectance equation

$$\Delta T = \kappa^{-1} \frac{\Delta R}{R}.$$

Manuscript received October 29, 2013; revised November 28, 2013; accepted November 29, 2013. Date of current version July 7, 2014.
Corresponding author: C. W. Leung (e-mail: apleung@polyu.edu.hk).
Digital Object Identifier 10.1109/TMAG.2013.2293780

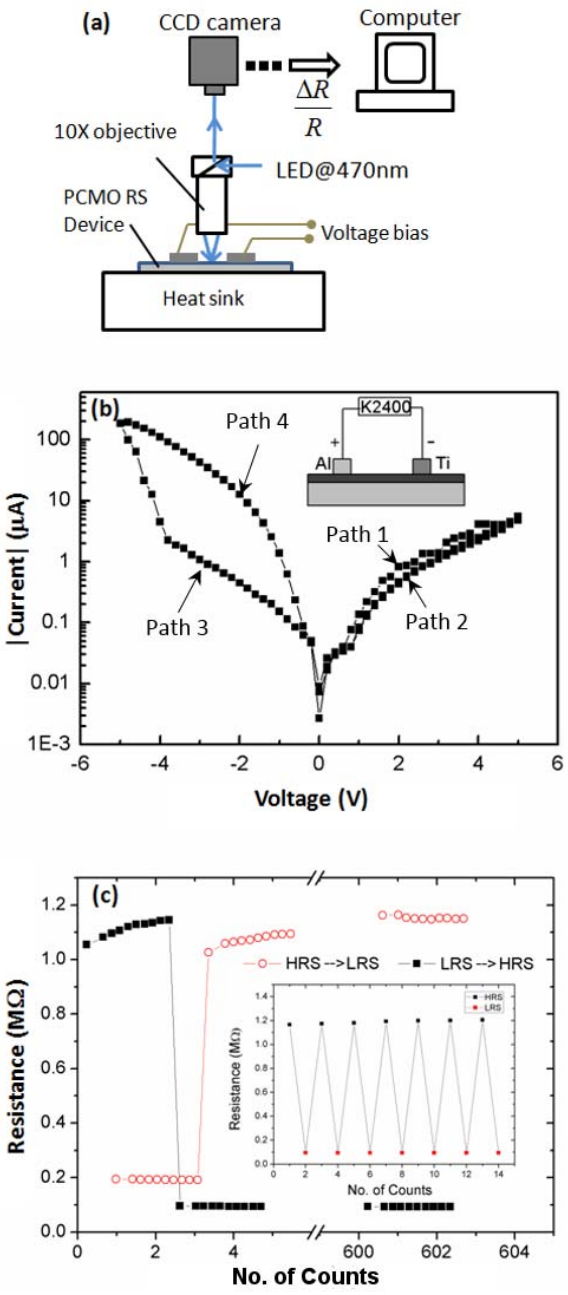

Fig. 1. (a) Schematic diagram of the thermoreflectance experimental setup. (b) Log scale I–V characteristics of the device under test. Inset: the polarity of the electrodes under positive bias. (c) Endurance data of the device under test both from LRS to HRS and HRS to LRS. Inset: the stability of the two resistance states.

In the above equation, $\Delta R/R$ is the normalized variation of reflectivity, and κ is the proportionality constant known as thermoreflectance coefficient, which is dependent on the illuminating wavelength and the material [22]. The measured thermoreflectance signal was transferred to a personal computer equipped with LabView for data analysis.

The devices under test contained 250 nm PCMO perovskite thin films epitaxially grown on $LaAlO_3$ (001) single crystal substrates, prepared by pulsed laser deposition (PLD) [23]. The substrates temperature and oxygen pressure during deposition were maintained at 650 °C and 150 mtorr, respectively.

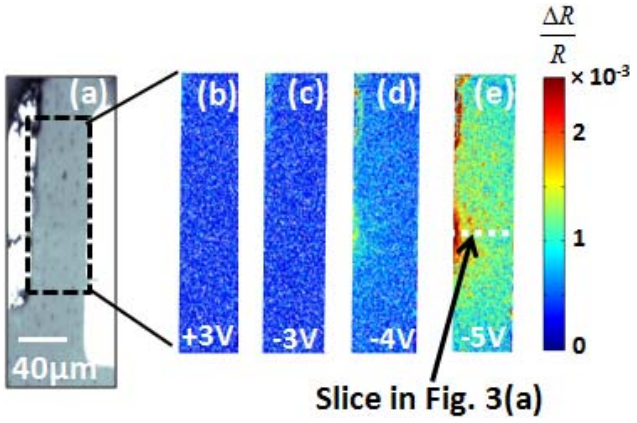

Fig. 2. (a) Optical image of the PCMO device under test. Thermoreflectance images of the sample at different bias levels, (b) +3, (c) −3, (d) −4, and (e) −5 V.

Square metal electrodes (Al and Ti) were prepared on PCMO by PLD through photolithography-prepared lift-off patterns, and electrical measurements (I–V characteristics and RS measurements) were performed with a Keithley 2400 sourcemeter. The positive current in the curve is defined as electric current flowing from Al to Ti.

III. Results and Discussion

The I–V characteristic of the device is shown in Fig. 1(b). When the applied voltage bias is increased from zero to +5V (path 1), the slope of the I–V curve is gentle. The same trend is followed along paths 2 and 3, until a −3.8 V bias is applied across the electrodes, which is accompanied by a sharp increase in current and the large current trend remains along path 4. Similar asymmetric I–V behavior is commonly observed in bipolar RS devices [24], [25]. By comparing the current values under HRS and LRS in Fig. 1(b), a resistance ratio between the HRS and LRS equals to 27 for the device under a −2 V probing voltage was obtained.

Stability and repeatability of the LRS and HRS in the devices have been confirmed, and the results are shown in Fig. 1(c). The resistance of the device was obtained by a probing voltage of −2 V. In the stability test, the device was first driven from LRS (HRS) to HRS (LRS) through the application of +5 V (−5 V) voltage pulse of 100 ms. The device was then disconnected from the measurement circuit for 10 min, before the resistance was probed again. No drastic change in the resistance value can be observed, demonstrating the nonvolatile nature of the resistance states. Repeated pulsing between the HRS and the LRS inset of Fig. 1(c) with +5 and −5 V pulses indicated that such states can be achieved for many times.

The optical image of an Al/PCMO/Ti device is shown in Fig. 2(a), and the corresponding thermoreflectance images under different bias conditions are shown in Fig. 2(b)–(e). The thermal images are taken while modulating the voltage bias across RS device at 10 Hz. The thermoreflectance coefficients of Al, Ti, and PCMO calibrated by microthermocouple are 3×10^{-4}, 8×10^{-4}, and 1.3×10^{-3} K^{-1}, respectively. The images can be converted into temperature

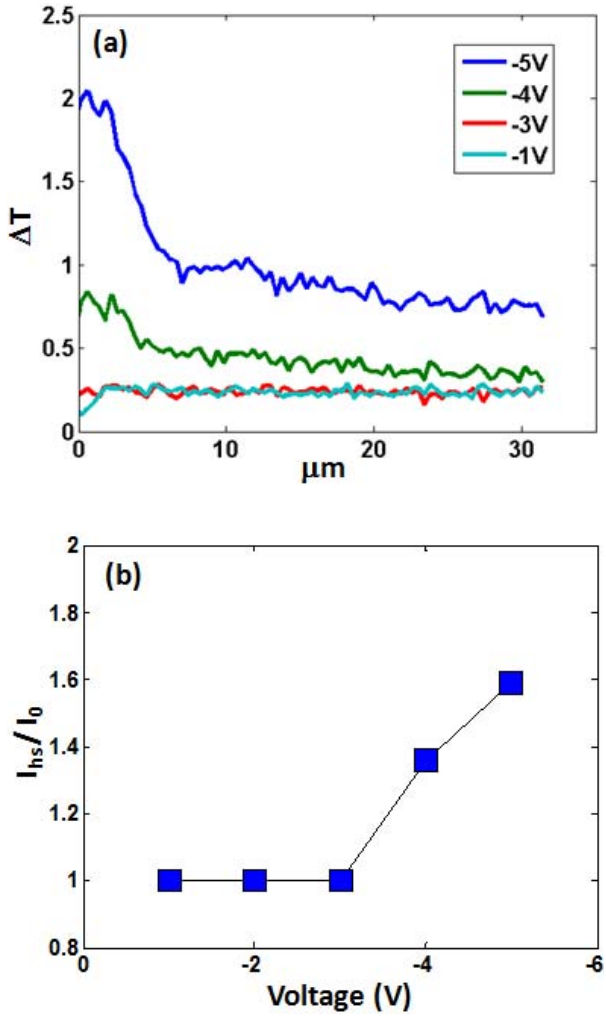

Fig. 3. (a) Temperature variation across the PCMO channel [the dotted line in Fig. 2(e)] under different bias levels. (b) Current ratio between the hot spot (I_{hs}) and the surrounding regions (I_0).

maps, by multiplying the thermoreflectance signals ($\Delta R/R$) for different materials by the corresponding thermoreflectance coefficients (κ). As we are only comparing the temperature of the same material, for simplicity, only the thermoreflectance signals ($\Delta R/R$) are shown in Fig. 2(b)–(e).

At positive bias [Fig. 2(b)], the thermoreflectance signal within the device is spatially homogenous, and no significant localized heating can be observed as the current passing though the device is very small at the HRS. At low negative bias levels up to -3 V [Fig. 2(c)], the thermoreflectance signal remains nearly the same as in the positive bias regime, and no heating is observed. However, when the applied voltage is increased to -4 V [Fig. 2(d)], localized hot spots start forming at the PCMO edge next to the Al electrode. If the bias voltage is further increased to -5 V [Fig. 2(e)], stronger localized heating occurs and the hot spots grow in size. From Fig. 2(e), two localized hot spots can be clearly observed, and the heated region spans over a distance of 10 μm along the edge of the Al electrode.

The horizontal averaged temperature variation of the PCMO channel at various voltage biases are compared in Fig. 3(a). The temperature gradient across the hot spot is about 2×10^5 K/m at -5 V bias, and it represents a significant amount of heat flowing from the Al to Ti through the PCMO. Since such localized heating phenomenon occurs only under large negative bias, it suggests that uneven current injection occurs when the device is at LRS. Assuming that the heat is generated by Joule heating, the uniformity of the injected current can be estimated by $(\Delta T_1/\Delta T_2) = (I_1/I_2)^2$. The ratio between the current injection at the hot spot (I_{hs}) and the surrounding region (I_0) under different bias levels is shown in Fig. 3(b). It can be observed that the current injection on the hot spot is 60% more than the surrounding region at -5 V bias.

In the current planar PCMO devices, hot spots were observed instead of a hot filament path. This is quite different from the recent finding by Janousch *et al.* [26] on Cr-doped $SrTiO_3$ single crystal planar RS devices, where hot filament path due to oxygen vacancies were observed. This is believed due to the large current passing though the single crystal device, leading to significant bulk Joule heating effect. The observation of the hot spots in the current finding indicates uneven current injection from the Al to the PCMO interface at the LRS. The measured temperature variation of the Ti electrode is much smaller than the Al electrode, and no hot filament path is observed in the PCMO thin film when RS occurs. These indicate the current is evenly distributed in the PCMO thin film and the Ti electrode. It suggests the origin of the RS should be located at the interface between the Al and PCMO.

The thermal images observation agrees with the recent findings by the others in the capacitor-like structure RS devices, where AlO_x layer is formed underneath the Al electrode. The formation and deformation of the AlO_x layer has shown to be related to the RS mechanisms of the device [24], [25], [27]. At HRS, AlO_x layer is formed at the Al/PCMO interface and the current passing though the device is small. When the device switches to LRS, deformation of the AlO_x layer starts to occur, hence a larger current can pass though. The formation and deformation of the AlO_x is believed to be related to the chemical reaction between the Al electrode and O^{2-} from the PCMO [25]. The observed hot spots can arise from the uneven dissolution of the AlO_x layer while the device is switched from the HRS to LRS, resulting in the current crowding at the region without AlO_x. The nondestructive, *in-situ* current profiling method by thermoreflectance measurement supplements the electrical measurements to provide a more complete picture of the switching effect.

IV. Conclusion

In conclusion, planar perovskite-based bipolar RS devices with Al and Ti electrodes have been fabricated by PLD and investigated by thermoreflectance measurement. The nonuniform current injection in the planar PCMO RS device has been quantified by the high-resolution thermal imaging method. For the Al/PCMO/Ti planar device under test, it has been shown that the uneven current injection at the Al/PCMO interface is related to the RS mechanism of the device. The unevenness of the injected current from Al to the PCMO can be as large as 1.6 at -5 V bias. As the uneven current injection is difficult to

be characterized by electrical measurements, thermal imaging provides a versatile method to characterize the performance of the RS devices. The technique should be applicable to both bipolar and unipolar switching device structures.

ACKNOWLEDGMENT

This work was supported in part by UGC and in part by HKSAR under Grant PolyU 5013/08P, Grant PolyU 5112/08E, and Grant PolyU A-PM21/G-YN08/H-ZDAC. The work of Z. Luo was supported in part by the Fundamental Research Funds for the Central Universities under Grant 21612416 and in part by the National Science Foundation of China under Grant 11204105. P. K. L. Chan would like to thank Dr. D. Lüerßen for the fruitful discussion and help at the beginning of developing the thermoreflectance setup.

REFERENCES

[1] S. Q. Liu, N. J. Wu, and A. Ignatiev, "Electric-pulse-induced reversible resistance change effect in magnetoresistive films," *Appl. Phys. Lett.*, vol. 76, no. 19, pp. 2749–2753, 2000.

[2] A. Baikalov, Y. Q. Wang, B. Shen, B. Lorenz, S. Tsui, Y. Y. Sun, *et al.*, "Field-driven hysteretic and reversible resistive switch at the Ag-$Pr_{0.7}Ca_{0.3}MnO_3$ interface," *Appl. Phys. Lett.*, vol. 83, pp. 957–983, Jul. 2003.

[3] D. Lee, D. J. Seong, F. Xiang, R. Dong, S. Oh, and H. Hwang, "Resistance switching of copper doped MoO_x films for nonvolatile memory applications," *Appl. Phys. Lett.*, vol. 90, no. 12, pp. 122104-1–122104-3, 2007.

[4] M. Cölle, M. Buchel, and D. M. de Leeuw, "Switching and filamentary conduction in non-volatile organic memories," *Org. Electron.*, vol. 7, no. 5, pp. 305–312, 2006.

[5] B. J. Choi, D. S. Jeong, S. K. Kim, C. Rohde, S. Choi, J. H. Oh, *et al.*, "Resistive switching mechanism of TiO_2 thin films grown by atomic-layer deposition," *J. Appl. Phys.*, vol. 98, pp. 033715-1–033715, Aug. 2005.

[6] S. Kim and Y.-K. Choi, "Resistive switching of aluminum oxide for flexible memory," *Appl. Phys. Lett.*, vol. 92, pp. 223508-1–223508-3, Jun. 2008.

[7] R. Dong, D. S. Lee, W. F. Xiang, S. J. Oh, D. J. Seong, S. H. Heo, *et al.*, "Reproducible hysteresis and resistive switching in metal-Cu_xO-metal heterostructures," *Appl. Phys. Lett.*, vol. 90, no. 4, pp. 042107-1–042107-3, 2007.

[8] M. Fujimoto, H. Koyama, Y. Nishi, and T. Suzuki, "Resistive switching properties of high crystallinity and low-resistance $Pr_{0.7}Ca_{0.3}MnO_3$ thin film with point-contacted Ag electrodes," *Appl. Phys. Lett.*, vol. 91, pp. 223504-1–223504-3, Nov. 2007.

[9] A. Ruotolo, C. Y. Lam, W. F. Cheng, K. H. Wong, and C. W. Leung, "High-quality all-oxide Schottky junctions fabricated on heavily doped Nb:$SrTiO_3$ substrates," *Phys. Rev. B*, vol. 76, no. 7, pp. 075122-1–075122-5, 2007.

[10] A. Ruotolo, C. W. Leung, C. Y. Lam. W. F. Cheng, K. H. Wong, and G. P. Pepe, "Unification of bulk and interface electroresistive switching in oxide systems," *Phys. Rev. B*, vol. 77, no. 23, pp. 233103-1–233103-4, 2008.

[11] R. Waser and M. Aono, "Nanoionics-based resistive switching memories," *Nature Mater.*, vol. 6, no. 11, pp. 833–840, 2007.

[12] A. Sawa, "Resistive switching in transition metal oxides," *Mater. Today*, vol. 11, no. 6, pp. 28–36, 2008.

[13] A. Sawa, T. Fujii, M. Kawasaki, and Y. Tokura, "Hysteretic current–voltage characteristics and resistance switching at a rectifying Ti/$Pr_{0.7}Ca_{0.3}MnO_3$ interface," *Appl. Phys. Lett.*, vol. 85, no. 18, pp. 4073–4075, 2004.

[14] K. Tsubouchi, I. Ohkubo, H. Kumigashira, M. Oshima, Y. Matsumoto, K. Itaka, *et al.*, "High-throughput characterization of metal electrode performance for electric-field-induced resistance switching in metal/$Pr_{0.7}Ca_{0.3}MnO_3$/metal structures," *Adv. Mater.*, vol. 19, no. 13, pp. 1711–1713, 2007.

[15] S. Li, Z. L. Liao, J. Li, J. L. Gang, and D. N. Zheng, "Resistive switching properties and low resistance state relaxation in Al/$Pr_{0.7}Ca_{0.3}MnO_3$/Pt junctions," *J. Phys. D, Appl. Phys.*, vol. 42, no. 4, pp. 045411-1–045411-6, 2009.

[16] S. H. Phark, R. Jung, Y. J. Chang, T. W. Noh, and D.-W. Kim, "Interfacial reactions and resistive switching behaviors of metal/NiO/metal structures," *Appl. Phys. Lett.*, vol. 94, no. 2, pp. 022906-1–022906-3, 2009.

[17] S. H. Chang, J. S. Lee, S. C. Chae, S. B. Lee, C. Liu, B. Kahng, *et al.*, "Occurrence of both unipolar memory and threshold resistance switching in a NiO film," *Phys. Rev. Lett.*, vol. 102, no. 2, pp. 026801-1–026801-5, 2009.

[18] H. K. Lau, C. W. Leung, W. H. Hu, and P. K. L. Chan, "Interfacial defects in resistive switching devices probed by thermal analysis," *J. Appl. Phys.*, vol. 106, no. 1, pp. 014504-1–014504-4, 2009.

[19] P. K. L. Chan, K. P. Pipe, Z. Mi, J. Yang, P. Bhattacharya, and D. Lüerßen, "Thermal relaxation time and heat distribution in pulsed InGaAs quantum dot lasers," *Appl. Phys. Lett.*, vol. 89, no. 1, pp. 011110-1–011110-3, 2006.

[20] P. K. L. Chan, K. P. Pipe, G. Qin, and Z. Ma, "Thermoreflectance imaging of current dynamics in high power SiGe heterojunction bipolar transistors," *Appl. Phys. Lett.*, vol. 89, no. 23, pp. 233521-1–233521-3, 2006.

[21] D. Lüerßen, R. J. Ram, A. Hohl-AbiChedid, E. Clausen, and J. A. Hudgings, "Thermal profiling: Locating the onset of gain saturation in semiconductor optical amplifiers," *IEEE Photon. Technol. Lett.*, vol. 16, no. 7, pp. 1625–1627, Jul. 2004.

[22] G. Tessier, G. Jerosolimski, S. Hole, D. Fournier, and C. Filloy, "Measuring and predicting the thermoreflectance sensitivity as a function of wavelength on encapsulated materials," *Rev. Sci. Instrum.*, vol. 74, no. 1, pp. 495–499, 2003.

[23] Z. Luo and J. Gao, "Anomalous temperature and magnetic field dependences of current–voltage characteristics in $Pr_{0.6}Ca_{0.4}MnO_3$/Nb-doped $SrTiO_3$ heterojunctions," *J. Phys. D, Appl. Phys.*, vol. 43, no. 17, pp. 175003-1–175003-3, 2010.

[24] H. K. Lau, C. W. Leung, and Y. K. Chan, "Resistance switching properties of epitaxial $Pr_{0.7}Ca_{0.3}MnO_3$ thin films with different electrodes," *Phys. Status Solidi A*, vol. 206, no. 9, pp. 2182–2186, 2009.

[25] Z. L. Liao, Z. Z. Wang, Y. Meng, Z. Y. Liu, P. Gao, J. L. Gang, *et al.*, "Categorization of resistive switching of metal-$Pr_{0.7}Ca_{0.3}MnO_3$-metal devices," *Appl. Phys. Lett.*, vol. 94, no. 25, pp. 253503-1–253503-3, 2009.

[26] M. Janousch, G. I. Meijer, U. Staub, B. Delley, S. F. Karg, and B. P. Andreasson, "Role of oxygen vacancies in Cr-doped $SrTiO_3$ for resistance-change memory," *Adv. Mater.*, vol. 19, no. 17, pp. 2232–2235, 2007.

[27] D. J. Seong, M. Hassan, H. Choi, J. Lee, J. Yoon, J. B. Park, *et al.*, "Resistive-switching characteristics of Al/$Pr_{0.7}Ca_{0.3}MnO_3$ for nonvolatile memory applications," *IEEE Electron. Device Lett.*, vol. 30, no. 9, pp. 919–921, Sep. 2009.